

# Analytical Solution of Optimal Geometric Configuration Based on PDOP for DOA FDOA and TDOA

Junhua Yang, Hao Huan<sup>✉</sup>, Ran Tao

(School of Information and Electronics, Beijing Institute of Technology, Beijing 100081, China)

**Abstract:** The radar radiation source signals hold extremely high reconnaissance value. Accurately positioning these signals constitutes one of the key technologies in safeguarding the security of the electromagnetic space. The positioning error in multi-station scenarios is influenced not only by the accuracy of positioning parameter estimation but also by the geometric configuration of the positioning platform. This paper focuses on the direction of arrival (DOA), frequency difference of arrival (FDOA), and time difference of arrival (TDOA) methods, analyzing the optimal configuration, optimal detection area, and optimal position dilution of precision in both elevation-known and elevation-unknown scenarios. Specifically, the paper constructs a signal receiving model, establishes the corresponding positioning equations, and performs dimensional normalization on these equations to derive measurement values in meters. Through differential processing, the position dilution of precision is obtained, which is then used as the optimization function to determine the optimal configuration, optimal detection area, and optimal position dilution of precision. Simulation results validate the accuracy of the proposed formulas.

**Keywords:** optimal geometric configuration; analytical solution; position dilution of precision; direction of arrival (DOA); frequency difference of arrival (FDOA); time difference of arrival (TDOA)

## 1 Introduction

Onboard passive positioning technology offers advantages such as covert reconnaissance and unrestricted spatiotemporal detection, as it does not actively emit electromagnetic signals and satellite operations are not bounded by national borders [1, 2]. Additionally, compared to traditional radars, it features a broader detection range and longer detection distance. Consequently, it plays a pivotal role in modern electronic reconnaissance. Currently, common parameters used for locating radiation sources

include: direction of arrival (DOA), frequency of arrival (FOA)/frequency difference of arrival (FDOA), and time of arrival (TOA)/time difference of arrival (TDOA).

DOA estimation is achieved by resolving the phase differences of incident signals from different radiation sources. When the spacing between antenna elements in a linear array exceeds half a wavelength, algorithms such as multiple signal classification (MUSIC) and estimation of signal parameters via rotational invariance techniques (ESPRIT) may lead to ambiguities in the estimated DOA results [3]. The study in [4] addressed the phase ambiguity issue by gradually reducing the maximum element spacing. A key advantage of this method is that even the smallest element spacing can still be larger than half a wavelength. Additionally, Ref. [5] pro-

---

Manuscript received Aug. 5, 2025; revised Sep. 30, 2025; accepted Oct. 7, 2025. The associate editor coordinating the review of this manuscript was Dr. Junjie Wu. This work was supported by the National Natural Science Foundation of China (Nos. 62027801, 62301035).

✉ Corresponding author. Email: [huanhao@bit.edu.cn](mailto:huanhao@bit.edu.cn)

DOI: [10.15918/j.jbit1004-0579.2025.049](https://doi.org/10.15918/j.jbit1004-0579.2025.049)

posed a novel hybrid non-uniform linear array along with an effective DOA estimation scheme, which enables accurate discrimination of adjacent signal sources.

FOA determines the location of a radiation source based on the varying Doppler frequencies observed at different positions during relative motion [6]. Kalantari et al. [7] proposed using multiple position-related equations (at least two) derived from FOA measurements, combined with the Earth's surface equation, to locate unknown interference sources. Additionally, the study in [8] proposed a real-time method for estimating the position of radio frequency transmitters using multiple FDOA measurements, based on a polar coordinate geometric approach. For scenarios involving moving transmitters, C. Steffes et al. [9] developed a method to determine the FOA of information from automatic dependent surveillance-broadcast (ADS-B) transponders.

TOA/TDOA is a method for locating radiation sources by resolving the arrival times or time differences at receivers positioned at different locations [10]. A. Aubry et al. [11] investigated the observability conditions of the relative positions of a group of passive sensors based on TDOA and proposed an algorithm to calculate both the sensor positions and the source direction. For scenarios where measurement variance cannot be precisely known, the study in [12] evaluated the performance robustness of TOA and TDOA.

In addition to being affected by the accuracy of positioning parameter estimation, it has been found that the geometric configuration of receiving station locations determines the theoretical minimum value of positioning error [13]. Currently, there are two main approaches to achieving optimal geometric configuration. One is to derive the analytical solution of the optimal configuration through mathematical derivation based on the Cramér-Rao lower bound (CRLB) for position estimation [14, 15]. Such research has focused more on the TDOA positioning mecha-

nism [16], as its CRLB is relatively simple to formulate. The other approach is to convert it into a pure optimization problem, where the optimal receiver positions can be obtained with relatively low computational cost via classical optimization theory [17], search methods [18], genetic algorithms [19], swarm intelligence algorithms [20], and so on.

For the four-satellite positioning system under the constraint of parallel dual orbits, this paper derives analytical solutions for the DOA, FDOA, and TDOA positioning methods. It also obtains the optimal configuration, optimal detection area, and optimal position dilution of precision (PDOP), which is defined as the ratio of the positioning error to the measurement error in both scenarios where elevation is unknown and known.

## 2 Geometric Model

Fig. 1 shows a positioning geometric model. The coordinates of the stationary radar radiation source T in the east-north-up (ENU) coordinate system are expressed as  $\mathbf{P} = [x_0, y_0, z_0]^T$ . To simplify the analysis, a four-star positioning system with parallel dual-track constraints is considered. The center of the distributed platform is O, and the distance from each moving platform to the center O is D. To maintain a stable reconnaissance configuration, the speed of each platform is

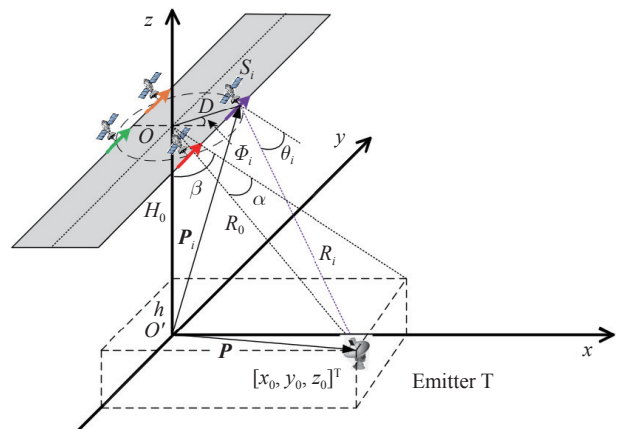


Fig. 1 Distributed synthetic aperture passive positioning geometric model

$\mathbf{V}_i = [0, v_0, 0]^T$ , and the position angles of the four platforms are  $\Phi = [\theta, -\theta, \pi - \theta, \theta - \pi]^T$ . Considering the height of the platform relative to the ground to be  $H_0$ , the distance from the distributed center to the radar radiation source is  $R_0 = \frac{H_0}{\cos \alpha \cos \beta}$ , where the pitch angle of the radar radiation source is  $\beta$ , and the azimuth angle is  $\alpha$ . Then,  $x_0 = H_0 \tan \beta$ ,  $y_0 = \frac{H_0}{\cos \beta} \tan \alpha$ ,  $z_0 = h$ ,  $x_i = D \cos \Phi_i$ ,  $y_i = D \sin \Phi_i$ ,  $z_i = h + H_0$ .

### 3 Optimal Configuration of DOA

#### 3.1 DOA Method

Considering that the axis direction of the array antenna is aligned with the flight direction of the platform, the angle of the incident wave from the radar radiation source to the  $i$ -th antenna is denoted as

$$\theta_i = -\arcsin \left[ \frac{\mathbf{e}_i^T (\mathbf{P} - \mathbf{P}_i)}{\|\mathbf{P} - \mathbf{P}_i\|} \right] \quad (1)$$

where  $\mathbf{e}_i = \mathbf{V}_i/v_i = [e_{xi}, e_{yi}, e_{zi}]^T$  represents the axis direction of the array antenna.

Assuming the transmitted signal is a point-frequency signal, the array antenna comprises  $M$  elements. The signal received by the  $m$ -th element is expressed as

$$r_i(t) = s(t) \exp \left( j2\pi \frac{md}{\lambda} \sin \theta_i \right) \quad (2)$$

where  $t$  represents time,  $s(t)$  represents the transmitted radar pulse signal,  $\lambda$  represents the wavelength, and  $d$  represents the array element spacing.

Considering  $|s(t)|^2 = 1$ , the signal from the  $m$ -th element after interfering with the first element is

$$r_i(t) = \exp \left( j2\pi \frac{md}{\lambda} \sin \theta_i \right) \quad (3)$$

The signal in Eq. (3) is a single-frequency signal whose frequency is related to  $\theta_i$ . The  $\theta_i$  can be obtained

$$\hat{\theta}_i = \arcsin \left[ \frac{\hat{\omega}_i \lambda}{2\pi d} \right] \quad (4)$$

where digital frequency  $\hat{\omega}_i$  can be estimated using fast Fourier transform (FFT).

The position of the radar radiation source is obtained by solving the positioning as follows

$$\frac{\mathbf{e}_i^T (\mathbf{P} - \mathbf{P}_i)}{\|\mathbf{P} - \mathbf{P}_i\|} = -\sin \hat{\theta}_i \quad (5)$$

#### 3.2 Position Dilution of Precision

Considering that the positioning Eq. (5) is established on the angles, and the dimensions between the angles and the unknown position of the radar radiation source are different, in order to integrate the dimensions, the reference range  $R_{\text{ref}}$  is introduced. Both sides of the positioning Eq. (5) are multiplied by  $R_{\text{ref}}$  at the same time and the observed quantity is the pseudo-azimuth range  $\hat{A}_i = -R_{\text{ref}} \sin \hat{\theta}_i$ . The positioning equation is

$$\frac{\mathbf{e}_i^T (\mathbf{P} - \mathbf{P}_i)}{\|\mathbf{P} - \mathbf{P}_i\|} R_{\text{ref}} = \hat{A}_i \quad (6)$$

Taking into account the observation error of pseudo-azimuth range, differentiating Eq. (6) can yield

$$\mathbf{G} \Delta_P = \Delta_A \quad (7)$$

where  $\mathbf{G}$  is a geometric matrix,  $\mathbf{G}(i, s) = \frac{R_{\text{ref}}}{\|\mathbf{P} - \mathbf{P}_i\|} \left[ e_{si} - \frac{(\mathbf{P} - \mathbf{P}_i)^T \mathbf{e}_i (s - s_i)}{\|\mathbf{P} - \mathbf{P}_i\|^2} \right]$ ,  $s = x, y, z$ ,  $\Delta_P = [dx \ dy \ dz]^T$ ,  $\Delta_A = [d\hat{A}_1 \ d\hat{A}_2 \ \dots \ d\hat{A}_L]^T$ .

The weight coefficient matrix can be used to describe the linear mapping relationship between the covariance matrix of the observed quantities and that of the evaluated quantities. The weight coefficient matrix is

$$\mathbf{H} = (\mathbf{G}^T \mathbf{G})^{-1} \quad (8)$$

The position dilution of precision is

$$\text{PDOP} = \sqrt{\text{tr}(\mathbf{H})} \quad (9)$$

where  $\text{tr}(\mathbf{H})$  represents the trace of matrix  $\mathbf{H}$ .

### 3.3 Optimal Configuration

#### 3.3.1 Elevation Unknown

Generally,  $D \ll R_0$ , and at this time,

$\|\mathbf{P} - \mathbf{P}_i\| \approx R_0$ . Considering three dimensional (3-D) positioning (scene 1),  $g_0 = D/H_0$  represents the distributed aperture coefficient, then

$$\mathbf{G}^T \mathbf{G} = \begin{bmatrix} G_{11} & G_{12} & G_{13} \\ G_{21} & G_{22} & G_{23} \\ G_{31} & G_{32} & G_{33} \end{bmatrix} \quad (10)$$

where  $G_{ij} = \sum_{k=1}^L G(k, i)G(k, j)$ ,  $G(i, 1) = -(\sin \alpha - g_0 \cos \alpha \cos \beta \sin \Phi_i) (\sin \beta - g_0 \cos \beta \cos \Phi_i) \cos \alpha$ ,  $G(i, 2) = (\sin \beta - g_0 \cos \beta \cos \Phi_i)^2 \cos^2 \alpha + (\cos \alpha \cos \beta)^2$ ,  $G(i, 3) = (\sin \alpha - g_0 \cos \alpha \cos \beta \sin \Phi_i) \cos \alpha \cos \beta$ .

Set  $\alpha = 0$ . Considering the main item, the position dilution of precision is

$$\text{PDOP}_1(\beta, \Theta; g_0) = \sqrt{\frac{4}{Lg_0^4 \sin^2 2\Theta \cos^6 \beta}} \quad (11)$$

where  $\text{PDOP}_1(\beta, \Theta; g_0)$  is monotonically decreasing with respect to  $\sin^2 2\Theta$  and  $\cos^2 \beta$ . Then,  $\Theta = \pi/4$ ,  $\beta = 0$ . The optimal position dilution of precision is

$$\text{PDOP}_1 = \frac{2}{g_0^2 \sqrt{L}} \quad (12)$$

Set  $\beta = 0$ . Considering the main item, position dilution of precision is

$$\text{PDOP}_1(\alpha, \Theta; g_0) = \sqrt{\frac{\cos^4 \alpha \sin^2 \Theta + \sin^2 \alpha \cos^2 2\Theta}{Lg_0^2 \sin^2 \alpha \cos^6 \alpha \sin^2 2\Theta \cos^2 \Theta}} \quad (13)$$

$$\begin{cases} (\cos^4 \alpha - \sin^2 \alpha) \sin^4 \Theta + 2 \sin^2 \alpha \sin^2 \Theta - \sin^2 \alpha = 0 \\ 2 \sin^2 \Theta \cos^6 \alpha - \cos^4 \alpha + 2 \cos^2 \Theta \cos^2 \alpha - \cos^2 \Theta = 0 \end{cases} \quad (14)$$

Take the derivatives of the intermediate variables  $\sin^2 \Theta$  and  $\cos^2 \alpha$ , and obtain the equations where the derivatives are equal to zero.

Substitute  $\cos^2 \Theta = 1 - \sin^2 \Theta$  and  $\sin^2 \alpha = 1 - \cos^2 \alpha$  into Eq. (14), eliminate  $\sin^2 \Theta$  and simplify, to obtain an equation about the variable  $u = \cos^2 \alpha$

$$4u^4 - 3u^3 - 2u^2 + 3u - 1 = 0 \quad (15)$$

which has two real solutions. Since  $u \in [0, 1]$ , we have  $\cos^2 \alpha = 0.655$ , which leads to  $\alpha = 36^\circ$ , and  $\sin^2 \Theta = (2u^2 - 4u + 2)/(u^3 + 2u^2 - 4u + 2) = 0.472$ , resulting in  $\Theta = 43^\circ$ . At this point, the optimal

position dilution of precision is

$$\text{PDOP}_1 = \frac{3.990}{g_0 \sqrt{L}} \quad (16)$$

By comparing Eqs. (12) and (16), it can be seen that when  $g_0 < 0.501$ , the optimal configuration parameters are  $\Theta = 43.39^\circ$ ,  $\beta = 0$ ,  $\alpha = 35.97^\circ$ , and the optimal position dilution of precision is  $\text{PDOP}_1 \approx 3.990/(g_0 \sqrt{L})$ .

### 3.3.2 Elevation Known

Considering 3-D positioning with known elevation (scene 2), set  $\alpha = 0$ . Considering the main item, position dilution of precision is

$$\text{PDOP}_2(\beta, \Theta; g_0) = \sqrt{\frac{4}{Lg_0^2 \sin^2 \Theta \sin^2 2\beta}} \quad (17)$$

where  $\text{PDOP}_2(\beta, \Theta; g_0)$  is monotonically decreasing with respect to  $\sin^2 \Theta$  and  $\sin^2 2\beta$ . Then,  $\Theta = \pi/2$ ,  $\beta = \pi/4$ . The optimal position dilution of precision is

$$\text{PDOP}_2 = \frac{2}{g_0 \sqrt{L}} \quad (18)$$

Set  $\beta = 0$ . Considering the main item, position dilution of precision is

$$\text{PDOP}_2(\alpha, \Theta; g_0) = \sqrt{\frac{4}{Lg_0^2 \cos^2 \Theta \sin^2 2\alpha}} \quad (19)$$

where  $\text{PDOP}_2(\alpha, \Theta; g_0)$  is monotonically decreasing with respect to  $\cos^2 \Theta$  and  $\sin^2 2\alpha$ . Then,  $\Theta = 0$ ,  $\alpha = \pi/4$ . The optimal position dilution of precision is shown in Eq. (18).

Therefore, it can be seen that the optimal configuration parameters are  $\Theta = \pi/2$ ,  $\beta = \pi/4$ ,  $\alpha = 0$  or  $\Theta = 0$ ,  $\beta = 0$ ,  $\alpha = \pi/4$ , and the optimal position dilution of precision is  $\text{PDOP}_2 \approx 2/(g_0 \sqrt{L})$ .

## 4 Optimal Configuration of FDOA

### 4.1 FDOA Method

The Doppler frequency from the radar radiation source to the  $i$ -th antenna is

$$f_i = \frac{\mathbf{V}_i^T (\mathbf{P} - \mathbf{P}_i)}{\lambda \|\mathbf{P} - \mathbf{P}_i\|} \quad (20)$$

Considering non-coherent frequency differ-

ence is  $f_p$  and the transmitted signal is a single-frequency signal with a carrier frequency of  $f_c$ , the signal received by the  $i$ -th antenna is

$$r_i(t) = \exp(j2\pi f_i t + j2\pi f_p t) \quad (21)$$

The signal in Eq. (21) is a single-frequency signal whose frequency is related to  $\mathbf{P}$ . Then positioning equation is

$$\frac{\mathbf{V}_i^T(\mathbf{P} - \mathbf{P}_i)}{\lambda \|\mathbf{P} - \mathbf{P}_i\|} + f_p = \hat{f}_i \quad (22)$$

Taking the first platform as the reference, the frequency difference between the  $i$ -th platform and the first platform is

$$\frac{\mathbf{V}_i^T(\mathbf{P} - \mathbf{P}_i)}{\lambda \|\mathbf{P} - \mathbf{P}_i\|} - \frac{\mathbf{V}_1^T(\mathbf{P} - \mathbf{P}_1)}{\lambda \|\mathbf{P} - \mathbf{P}_1\|} = \Delta \hat{f}_i \quad (23)$$

where  $\Delta \hat{f}_i = \hat{f}_{i+1} - \hat{f}_1$ .

The positioning results of Eqs. (22) and (23) are the same. Considering that there is a correlation among the frequency difference measurements in Eq. (23), for the convenience of the subsequent derivation of the error formula, Eq. (22) is selected as the positioning equation for FDOA.

## 4.2 Position Dilution of Precision

In order to integrate the dimensions, the reference Doppler frequency  $f_{\text{ref}} = v_{\text{ref}}/\lambda$  and the reference range  $R_{\text{ref}}$  are introduced. Both sides of the positioning Eq. (22) are multiplied by  $R_{\text{ref}}/f_{\text{ref}}$  at the same time, the fixed deviation of the pseudo-azimuth range caused by  $f_p$  is  $A_p = R_{\text{ref}}f_p/f_{\text{ref}}$ , and the observed quantity is the pseudo-azimuth range  $\hat{A}_i = R_{\text{ref}}\hat{f}_i/f_{\text{ref}}$ . The positioning equation is

$$\frac{\mathbf{V}_i^T(\mathbf{P} - \mathbf{P}_i)}{\lambda \|\mathbf{P} - \mathbf{P}_i\|} \frac{R_{\text{ref}}}{f_{\text{ref}}} + A_p = \hat{A}_i \quad (24)$$

Taking into account the observation error of pseudo-azimuth range, differentiating Eq. (7), we can yield

$$\mathbf{G}\Delta_P = \Delta_A \quad (25)$$

where  $\mathbf{G} = [\mathbf{G}_1 \ \mathbf{G}_2]$  is a geometric matrix,  $\mathbf{G}_1(i, s) = \frac{R_{\text{ref}}v_i}{\lambda f_{\text{ref}}\|\mathbf{P} - \mathbf{P}_i\|} \left[ \frac{v_{si}}{v_i} - \frac{(\mathbf{P} - \mathbf{P}_i)^T \mathbf{V}_i (s - s_i)}{v_i \|\mathbf{P} - \mathbf{P}_i\|^2} \right]$ ,  $s = x, y, z$ ,  $\mathbf{G}_2 = [1, 1, \dots, 1]^T$ ,  $\Delta_P = [dx \ dy \ dz \ dA_p]^T$ ,  $\Delta_A = [d\hat{A}_1 \ d\hat{A}_2 \ \dots \ d\hat{A}_L]^T$ ,  $\mathbf{V}_i = [v_{xi}, v_{yi}, v_{zi}]^T$ .

The weight coefficient matrix is

$$\mathbf{H} = (\mathbf{G}^T \mathbf{G})^{-1} = \begin{bmatrix} \mathbf{H}_{11} & \mathbf{H}_{12} \\ \mathbf{H}_{21} & \mathbf{H}_{22} \end{bmatrix} \quad (26)$$

Position dilution of precision is

$$\text{PDOP} = \sqrt{\text{tr}(\mathbf{H}_{11})} \quad (27)$$

## 4.3 Optimal Configuration

### 4.3.1 Elevation Unknown

With the reference Doppler frequency set as  $f_{\text{ref}} = v_0/\lambda$  and the reference detection distance as  $R_{\text{ref}} = R_0$ , consider 3-D positioning (scene 1), and then

$$\mathbf{G}^T \mathbf{G} = \begin{bmatrix} G_{11} & G_{12} & G_{13} & G_{14} \\ G_{21} & G_{22} & G_{23} & G_{24} \\ G_{31} & G_{32} & G_{33} & G_{34} \\ G_{41} & G_{42} & G_{43} & G_{44} \end{bmatrix} \quad (28)$$

where  $G_{ij} = \sum_{k=1}^L G(k, i)G(k, j)$ ,  $G(i, 1) = -(\sin \alpha - g_0 \cos \alpha \cos \beta \sin \Phi_i) (\sin \beta - g_0 \cos \beta \cos \Phi_i) \cos \alpha$ ,  $G(i, 2) = (\sin \beta - g_0 \cos \beta \cos \Phi_i)^2 \cos^2 \alpha + (\cos \alpha \cos \beta)^2$ ,  $G(i, 3) = (\sin \alpha - g_0 \cos \alpha \cos \beta \sin \Phi_i) \cos \alpha \cos \beta$ ,  $G(i, 4) = 1$

Set  $\alpha = 0$ , so the position dilution of precision is

$$\text{PDOP}_1(\beta, \Theta; g_0) = \sqrt{\frac{a_1 + b_1 + c_1}{d_1}} \quad (29)$$

where  $a_1 = 4 \sin^2 \beta \sin^2 \Theta$ ,  $b_1 = 4 g_0^2 \sin^2 \beta \cos^2 \beta \sin^2 \Theta \cos^2 \Theta$ ,  $c_1 = g_0^2 \sin^4 \Theta \cos^4 \beta$ ,  $d_1 = 4 L g_0^4 \sin^4 \Theta \cos^2 \Theta \sin^2 \beta \cos^6 \beta$ .

Taking the partial derivatives of  $\text{PDOP}_1(\beta, \Theta; g_0)$  in Eq. (29) with respect to the variables  $\sin^2 \Theta$  and  $\sin^2 \beta$ , equations with derivatives equal to zero are obtained.

$$\begin{cases} \sin^2 \Theta = \frac{-b + \sqrt{ab}}{a - b} \\ \sin^2 \beta = \frac{\sqrt{24 - 27 \sin^2 \Theta}}{6} g_0 \end{cases} \quad (30)$$

where  $a = g_0^2 \cos^4 \beta + 4 \sin^2 \beta$ ,  $b = 4 \sin^2 \beta + 4 g_0^2 \sin^2 \beta \cos^2 \beta$ .

We have  $\Theta = \pi/4$ ,  $\beta = \arcsin \sqrt{0.54 g_0}$ . The optimal positioning error is

$$\text{PDOP}_1 \approx \frac{2}{g_0^2 \sqrt{L(1 - 0.54 g_0)^3}} \quad (31)$$

Set  $\beta = 0$ ,  $\det(\mathbf{G}^T \mathbf{G}) = 0$ , the position accuracy dilution factor is infinite, and then positioning is impossible.

### 4.3.2 Elevation Known

Considering 3-D positioning with known elevation (scene 2), set  $\alpha = 0$ . Considering the main item, position dilution of precision is

$$\text{PDOP}_2(\beta, \Theta; g_0) = \sqrt{\frac{4 \cos^2 \Theta + \sin^2 \Theta}{L g_0^2 \sin^2 2\beta \sin^2 \Theta \cos^2 \Theta}} \quad (32)$$

where  $\text{PDOP}_2(\beta, \Theta; g_0)$  is monotonically decreasing with respect to  $\sin^2 2\beta$ , thus  $\beta = \pi/4$ . Taking the partial derivative with respect to  $\sin^2 \Theta$  and setting it to 0 gives

$$3 \sin^4 \Theta - 8 \sin^2 \Theta + 4 = 0 \quad (33)$$

The solution that satisfies the constraints of the actual scenario for this equation is  $\sin \Theta = \sqrt{2/3}$ . Further,  $\Theta = 54.74^\circ$ . At this point, the optimal position dilution of precision is

$$\text{PDOP}_2 = \frac{3}{g_0 \sqrt{L}} \quad (34)$$

Set  $\beta = 0$ ,  $\det(\mathbf{G}^T \mathbf{G}) = 0$ , the position accuracy dilution factor is infinite, and then positioning is impossible.

## 5 Optimal Configuration of TDOA

### 5.1 TDOA Method

The instantaneous distance between the radar radiation source and the platform is

$$R_i = \|\mathbf{P} - \mathbf{P}_i\| \quad (35)$$

The signal received by the  $i$ -th antenna is

$$r_i(t) = s\left(t - \Delta t - \frac{R_i}{c}\right) \quad (36)$$

where  $s(t)$  represents the transmitted signal,  $c$  represents the speed of light and  $\Delta t$  represents a fixed delay.

By performing correlation processing on the transmitted signal and the received signal in Eq. (36), the estimated value of the time delay  $\hat{t}_i$  corresponding to the correlation peak can be obtained. Then positioning equation is

$$\frac{\|\mathbf{P} - \mathbf{P}_i\|}{c_1} + \Delta t = \hat{t}_i \quad (37)$$

Taking the first platform as the reference, the difference time between the  $i$ -th platform and the first platform is

$$\frac{\|\mathbf{P} - \mathbf{P}_i\|}{c_1} - \frac{\|\mathbf{P} - \mathbf{P}_1\|}{c_1} = \Delta \hat{t}_i \quad (38)$$

where  $\Delta \hat{t}_i = \hat{t}_{i+1} - \hat{t}_1$ .

The positioning results of Eqs. (37) and (38) are the same. Considering that there is a correlation among the time difference measurements in Eq. (38), for the convenience of the subsequent derivation of the error formula, Eq. (37) is selected as the positioning equation for TDOA.

### 5.2 Position Dilution of Precision

Both sides of the positioning Eq. (37) are multiplied by  $c_1$  at the same time, the fixed deviation of the pseudo range caused by  $\Delta t$  is  $\Delta R = c_1 \Delta t$ , and the observed quantity is the pseudo range  $\hat{R}_i = c_1 \hat{t}_i$ . The positioning equation is

$$\|\mathbf{P} - \mathbf{P}_i\| + \Delta R = \hat{R}_i \quad (39)$$

Taking into account the observation error of pseudo-range, differentiating Eq. (39) can yield

$$\mathbf{G} \Delta_P = \Delta_R \quad (40)$$

where  $\mathbf{G} = [\mathbf{G}_1 \ \mathbf{G}_2]$  is a geometric matrix,  $\mathbf{G}_1(i, s) = \frac{s - s_i}{\|\mathbf{P} - \mathbf{P}_i\|}$ ,  $s = x, y, z$ ,  $\mathbf{G}_2(i) = [1, 1, \dots, 1]^T$ ,  $\Delta_P = [dx \ dy \ dz \ dR]^T$ ,  $\Delta_R = [d\hat{R}_1 \ d\hat{R}_2 \ \dots \ d\hat{R}_L]^T$ , and  $dR$  represents the estimated error of  $\Delta R$ .

The weight coefficient matrix is shown in Eq. (26). Position dilution of precision is shown in Eq. (27).

### 5.3 Optimal Configuration

#### 5.3.1 Elevation Unknown

The position dilution of precision is

$$\text{PDOP}_1(\alpha, \beta, \Theta; g_0) = \sqrt{\frac{H(1,1) + H(2,2) + H(3,3)}{\det(\mathbf{G}^T \mathbf{G})}} \quad (41)$$

where  $H(i, j)$  represents the element value of the  $i$ -th row and  $j$ -th column of  $H$ . Then

$$\mathbf{G}^T \mathbf{G} = \begin{bmatrix} G_{11} & G_{12} & G_{13} & G_{14} \\ G_{21} & G_{22} & G_{23} & G_{24} \\ G_{31} & G_{32} & G_{33} & G_{34} \\ G_{41} & G_{42} & G_{43} & G_{44} \end{bmatrix} \quad (42)$$

where  $G_{ij} = \sum_{k=1}^L G(k, i)G(k, j)$ ,  $G(i, 1) = \cos \alpha \sin \beta - g_0 \cos \alpha \cos \beta \cos \Phi_i$ ,  $G(i, 2) = \sin \alpha - g_0 \cos \alpha \cos \beta \sin \Phi_i$ ,  $G(i, 3) = -\cos \alpha \cos \beta$ ,  $G(i, 4) = 1 - g_0 \cos^2 \alpha \sin \beta \cos \beta \cos \Phi_i - g_0 \sin \alpha \cos \alpha \cos \beta \sin \Phi_i - g_0^2 \sin \alpha \cos^3 \alpha \sin \beta \cos^2 \beta \sin \Phi_i \cos \Phi_i$ .

Taking the partial derivative of  $\text{PDOP}_1(\alpha, \beta, \Theta; g_0)$  in Eq. (41) with respect to the variable  $\alpha, \beta, \Theta$ , the derivative is 0 and then we have  $\Theta = 45^\circ$ ,  $\beta = 35^\circ$ ,  $\alpha = 30^\circ$ . The optimal positioning error is

$$\text{PDOP}_1 = \frac{8}{5g_0^3 \sqrt{L}} \quad (43)$$

### 5.3.2 Elevation Known

Considering 3-D positioning with known elevation (scene 2), set  $\alpha = 0$ . Considering the main

item, position dilution of precision is

$$\text{PDOP}_2(\beta, \Theta; g_0) = \sqrt{\frac{\cos^2 \Theta + \sin^2 \Theta}{Lg_0^2 \cos^2 \beta \sin^2 \Theta \cos^2 \Theta}} \quad (44)$$

In Eq. (44), the parameter  $\text{PDOP}_2$  decreases monotonically with respect to the variable  $\cos^2 \beta$ , and then  $\beta = 0$ . Taking the partial derivative of  $\text{PDOP}_2$  with respect to  $\sin^2 \Theta$ , it equals zero and  $\Theta = 45^\circ$ . Thus, the optimal position dilution of precision is as Eq. (18).

## 6 Simulation Experiments

The estimated standard deviation of  $\hat{A}_i$  is  $\sigma_A$  and the estimated standard deviation of  $\hat{R}_i$  is  $\sigma_R$ . Set  $\sigma_A = \sigma_R = 1$  m. Fig. 2 illustrates the optimal results obtained by searching for PDOP. Specifically, Fig. 2(a) presents the optimal PDOP values with different  $g_0$  values. From Fig. 2(b), the

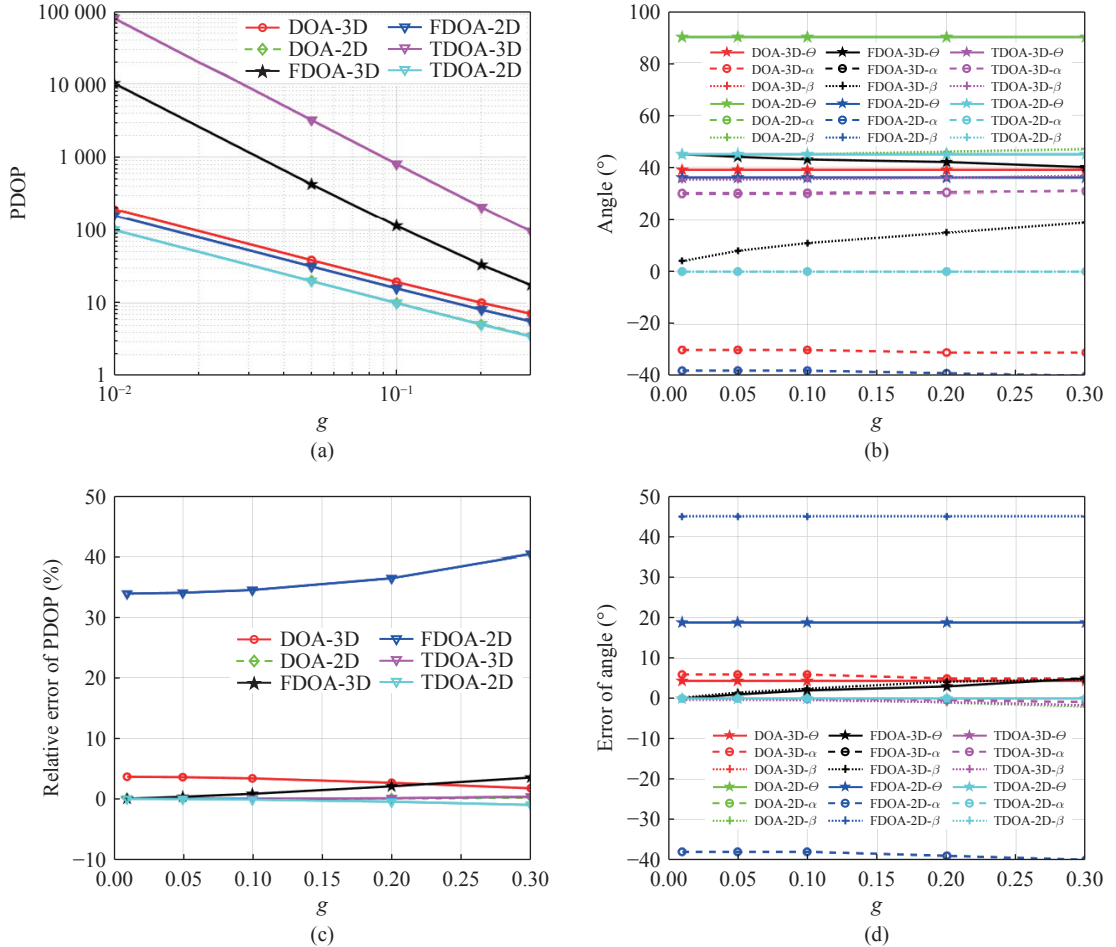


Fig. 2 Optimal results: (a) PDOP; (b) geometric configuration; (c) error of PDOP; (d) error of angle

optimized results of  $\Theta$  in the two scenarios via the three methods are  $39^\circ$ ,  $90^\circ$ ,  $43^\circ$ ,  $36^\circ$ ,  $45^\circ$ , and  $45^\circ$  respectively. This indicates that the optimal configuration for DOA-based two-dimensional positioning is linear, while for other cases, the optimal configuration is approximately square-shaped. Fig. 2(c) shows the relative error between the theoretical PDOP values and the actual searched true values. Except for FDOA-3D, the relative error of the analytical solution for the optimal PDOP is within 5%, which validates the accuracy of the theoretical formula. Fig. 2(d) displays the analytical solution errors of the configuration parameter  $\Theta$  and the radar radiation source location parameters  $\alpha$ ,  $\beta$ . Except for FDOA-3D, the optimal analytical solution errors of  $\alpha$ ,  $\beta$  and  $\Theta$  are within  $5^\circ$ , further confirming the accuracy of the theoretical formula.

Set  $g_0 = 0.1$ . Fig. 3 illustrates the PDOP values at various positions under the optimal configuration. Specifically, Fig. 3(a) presents the PDOP values corresponding to different radiation source locations in DOA-based three-dimensional positioning, where the optimal positioning area is observed to lie directly ahead of and directly behind the antenna axis. Fig. 3(b) displays the PDOP values for different radiation source locations in DOA-based two-dimensional positioning; here, the optimal positioning area is located on the positive side of the antenna axis, with a pitch angle of  $45^\circ$ . Fig. 3(c) shows the PDOP values for different radiation source locations in FDOA-based three-dimensional positioning, revealing that the optimal positioning area is along the direct path of the flight direction. Fig. 3(d) depicts the PDOP values of FDOA three-dimensional positioning across different radiation source locations, indicating that the optimal positioning area encompasses the front and rear directions of the flight path as well as the rear side. Additionally, there are local optimal detection areas on both the front and rear sides. Fig. 3(e) presents the PDOP values for

different radiation source locations in TDOA-based three-dimensional positioning, where the optimal positioning area is found in the oblique front and rear directions relative to the baseline. Fig. 3(f) shows the PDOP values for different radiation source locations in two-dimensional TDOA positioning, with the optimal positioning area identified at the ground point.

## 7 Conclusion

For the four-satellite positioning system under the constraint of parallel dual orbits, this paper derives analytical solutions for the DOA, FDOA, and TDOA positioning methods, along with the optimal configuration, optimal detection area, and optimal PDOP in both elevation-unknown and elevation-known scenarios. Simulation results validate the accuracy of the derived formulas. Specifically, the optimal configuration for DOA-based two-dimensional positioning is linear, while for other cases, the optimal configuration is approximately square-shaped.

## References:

- [1] M. Chen and J. Xu, "Application and development of modern electronic reconnaissance satellites," *Space International*, no. 10, pp. 16-18, 2001.
- [2] Q. Zhang, S. Li, B. Wu, and J. Wang, "Passive maritime surveillance based on low earth orbit satellite constellations," *IEEE Wireless Communications*, vol. 27, no. 6, pp. 61-67, 2020.
- [3] C. Tan, S. Foo, X. Mei, L. Liang, and T. A. Gulliver, "Ambiguity in music and esprit for direction of arrival estimation," *IEEE Sensors Journal*, vol. 38, no. 24, pp. 1598-1600, 2002.
- [4] K. Sundaram, R. Mallik, and U. Murthy, "Modulo conversion method for estimating the direction of arrival," *IEEE Transactions on Aerospace and Electronic Systems*, vol. 36, no. 4, pp. 1391-1396, 2000.
- [5] K. Aghababaiyan, V. Shah-Mansouri, and B. Maham, "High-precision OMP-based direction of arrival estimation scheme for hybrid non-uniform array," *IEEE Communications Letters*, vol. 24, no. 2, pp. 354-357, 2020.
- [6] D. J. Nelson and J. B. McMahon, "Target location

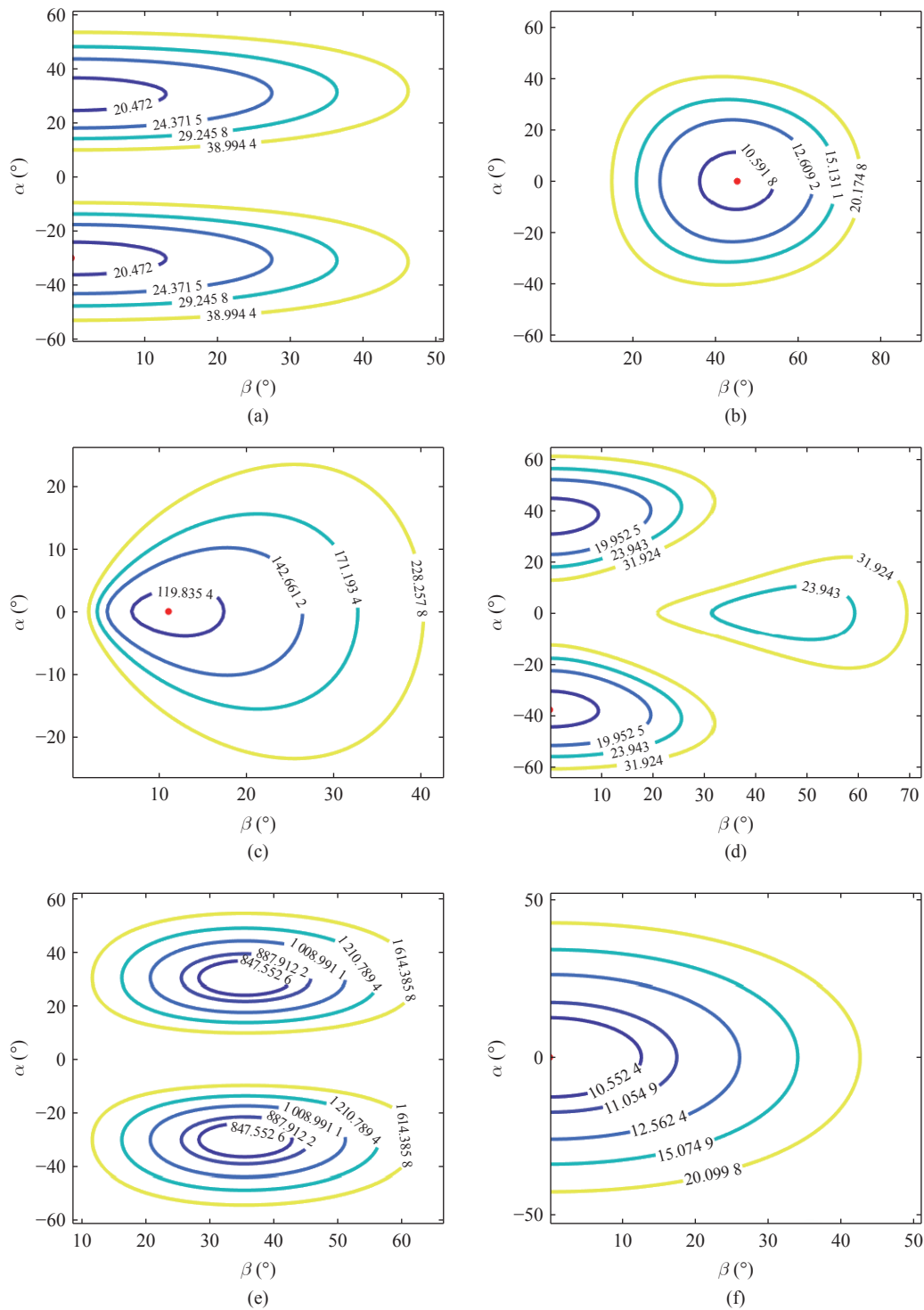


Fig. 3 PDOP of different positions with optimal  $\Theta$ : (a) by DOA in 3D scene; (b) by DOA in 2D scene; (c) by FDOA in 3D scene; (d) by FDOA in 2D scene; (e) by TDOA in 3D scene; (f) by TDOA in 2D scene

from the estimated instantaneous received frequency,” in *Proceedings of SPIE*, Orlando, Florida, United States, pp. 1-8, 2011.

[7] A. Kalantari, S. Maleki, S. Chatzinotas, and B. Ottersten, “Frequency of arrival-based interference localization using a single satellite,” in *2016 8th*

*Advanced Satellite Multimedia Systems Conference and the 14th Signal Processing for Space Communications Workshop (ASMS/SPSC)*, Palma de Mallorca, Spain, pp. 1-6, 2016.

[8] W. de Carvalho Rodrigues and J. Antonio Apolinario, “An emitter localization method based on

- multiple differential doppler measurements,” *IEEE Latin America Transactions*, vol. 20, no. 4, pp. 537-544, 2022.
- [9] C. Steffes and S. Rau, “FDOA determination of ADSB transponder signals,” in *2012 Workshop on Sensor Data Fusion: Trends, Solutions, Applications (SDF)*, Bonn, Germany, pp. 84-87, 2012.
- [10] J. Y. Do, M. Rabinowitz, and P. Enge, “Robustness of TOA and TDOA positioning under suboptimal weighting conditions,” *IEEE Transactions on Aerospace and Electronic Systems*, vol. 43, no. 3, pp. 1177-1180, 2007.
- [11] A. Aubry, V. Carotenuto, A. De Maio, and L. Pallotta, “Localization in 2D PBR with multiple transmitters of opportunity: A constrained least squares approach,” *IEEE Transactions on Signal Processing*, vol. 68, pp. 634-646, 2020.
- [12] L. Pallotta and G. Giunta, “Accurate delay estimation for multisensor passive locating systems exploiting the cross-correlation between signals cross-correlations,” *IEEE Transactions on Aerospace and Electronic Systems*, vol. 58, no. 3, pp. 2568-2576, 2022.
- [13] S. Joshi and S. Boyd, “Sensor selection via convex optimization,” *IEEE Transactions on Signal Processing*, vol. 57, no. 2, pp. 451-462, 2009.
- [14] B. Yang and J. Scheuing, “Cramer-rao bound and optimum sensor array for source localization from time differences of arrival,” in *Proceedings (ICASSP’05), IEEE International Conference on Acoustics, Speech, and Signal Processing, 2005*, Philadelphia, PA, USA, pp. 961-964, 2005.
- [15] Y. Bin and S. Jan, “A theoretical analysis of 2D sensor arrays for TDOA based localization,” in *2006 IEEE International Conference on Acoustics Speech and Signal Processing Proceedings (ICASSP)*, Toulouse, France, pp. 4571-4574, 2006.
- [16] M. Sadeghi, F. Behnia, and R. Amiri, “Optimal geometry analysis for TDOA-based localization under communication constraints,” *IEEE Transactions on Aerospace and Electronic Systems*, vol. 57, no. 5, pp. 3096-3106, 2021.
- [17] K. Panwar, G. Fatima, and P. Babu, “Optimal sensor placement for hybrid source localization using fused TOA-RSS-AOA measurements,” *IEEE Transactions on Aerospace and Electronic Systems*, vol. 59, no. 2, pp. 1643-1657, 2023.
- [18] S. Xu, Y. Ou, and X. Wu, “Optimal sensor placement for 3-D time-of-arrival target localization,”

*IEEE Transactions on Signal Processing*, vol. 67, no. 19, pp. 5018-5031, 2019.

- [19] P. Chiu and F. Lin, “A simulated annealing algorithm to support the sensor placement for target location,” in *Canadian Conference on Electrical and Computer Engineering 2004 (IEEE Cat. No. 04CH37513)*, Niagara Falls, ON, Canada, pp. 867-870, 2004.
- [20] P. Gou, B. He, and Z. Yu, “A node location algorithm based on improved whale optimization in wireless sensor networks,” *Wireless Communications and Mobile Computing*, vol. 2021, no. 1, pp. 7523938, 2021.



**Junhua Yang** received the B.E. degree in electronic information engineering from Beijing Institute of Technology, Beijing, China in 2019. He is currently working toward the Ph.D. degree in information and communication engineering with Beijing Institute of Technology, Beijing, China.



**Hao Huan** received the B.E. degree in information engineering from Zhengzhou University, Zhengzhou, China, in 2006, and the Ph.D. degree in information and communication engineering from Beijing Institute of Technology, Beijing, China, in 2013. He is currently an Assistant Professor with School of Information and Electronics, Beijing Institute of Technology. He was a Visiting Researcher with University of Delaware, Newark, DE, USA, in 2017. His research interests include wireless communication and emitter location.



**Ran Tao** received the B.S. degree in radar engineering from Electronic Engineering Institute of PLA, Hefei, in 1985 and the M.S. in communication and electronic systems and Ph.D. degrees in electromagnetic measurement technology and instrument from Harbin Institute of Technology, Harbin, in 1990 and 1993, respectively. In 2001, he was a Senior Visiting Scholar with University of Michigan, Ann Arbor, MI, USA. He is currently a Professor with School of Information and Electronics, Beijing Institute of Technology, Beijing, China. He has authored or coauthored three books and more than 100 peer-reviewed journal articles. His current research interests include fractional Fourier transform and its applications, theory, and technology for radar and communication systems.